



MODIS BIOPHYSICAL STATES AND NEXRAD PRECIPITATION IN A STATISTICAL EVALUATION OF ANTECEDENT MOISTURE CONDITION AND STREAMFLOW¹

B. P. Weissling and H. Xie²

ABSTRACT: The potential of remotely sensed time series of biophysical states of landscape to characterize soil moisture condition antecedent to radar estimates of precipitation is assessed in a statistical prediction model of streamflow in a 1,420 km² watershed in south-central Texas. Moderate Resolution Imaging Spectroradiometer (MODIS) time series biophysical products offer significant opportunities to characterize and quantify hydrologic state variables such as land surface temperature (LST) and vegetation state and status. Together with Next Generation Weather Radar (NEXRAD) precipitation estimates for the period 2002 through 2005, 16 raw and deseasoned time series of LST (day and night), vegetation indices, infrared reflectances, and water stress indices were linearly regressed against observed watershed streamflow on an eight-day aggregated time period. Time offsets of 0 (synchronous with streamflow event), 8, and 16 days (leading streamflow event) were assessed for each of the 16 parameters to evaluate antecedent effects. The model results indicated a reasonable correlation ($r^2 = 0.67$) when precipitation, daytime LST advanced 16 days, and a deseasoned moisture stress index were regressed against log-transformed streamflow. The estimation model was applied to a validation period from January 2006 through March 2007, a period of 12 months of regional drought and base-flow conditions followed by three months of above normal rainfall and a flood event. The model resulted in a Nash-Sutcliffe estimation efficiency (E) of 0.45 for flow series (in log-space) for the full 15-month period, -0.03 for the 2006 drought condition period, and 0.87 for the 2007 wet condition period. The overall model had a relative volume error of -32% . The contribution of parameter uncertainties to model discrepancy was evaluated.

(KEY TERMS: surface water hydrology; remote sensing; streamflow estimation; MODIS; NEXRAD.)

Weissling, B. P. and H. Xie, 2009. MODIS Biophysical States and NEXRAD Precipitation in a Statistical Evaluation of Antecedent Moisture Condition and Streamflow. *Journal of the American Water Resources Association* (JAWRA) 45(2):419-433. DOI: 10.1111/j.1752-1688.2009.00300.x

INTRODUCTION

Time series imagery from Earth Observation (EO) platforms such as that from the National Aeronautics and Space Administration's (NASA) Moderate Resolu-

tion Imaging Spectroradiometer (MODIS)/Terra and Aqua satellites offers substantial opportunity to describe the spatial and temporal heterogeneity of the landscape, in terms of biophysical processes and properties. In the development of distributed hydrologic models of watersheds, the provision of remotely

¹Paper No. JAWRA-08-0086-P of the *Journal of the American Water Resources Association* (JAWRA). Received May 18, 2008; accepted August 25, 2008. © 2009 American Water Resources Association. **Discussions are open until October 1, 2009.**

²Respectively, Adjunct Research Scientist, Department of Geological Sciences, University of Texas San Antonio, 1 UTSA Circle, San Antonio, Texas 78249 and Geophysicist, SWCA Environmental Consultants, 6200 UTSA Boulevard, Suite 102, San Antonio, Texas 78249; and Assistant Professor, Department of Geological Sciences, University of Texas San Antonio, 1 UTSA Circle, San Antonio, Texas 78249 (E-Mail/Weissling: bweissling@swca.com).

sensed data supports the parameterization of key hydrologic variables such as near surface soil moisture, surface temperature, vegetation cover, land use, and evapotranspiration. Ground-based remote sensing of precipitation provided by the Next Generation Weather Radar (NEXRAD) detects and quantifies precipitation at a spatial extent and resolution that cannot be provided by traditional rain gauge networks. As such, NEXRAD spatially-distributed precipitation estimates are now commonly included as forcing data in hydrologic prediction models (Carpenter *et al.*, 2001; Ajami *et al.*, 2004; Bedient *et al.*, 2004; Moon *et al.*, 2004; Kalinga and Gan, 2006; Segond *et al.*, 2007; Makkeasorn *et al.*, 2008). The spatial and temporal resolution of these operational ground and space-based remote sensing platforms can, therefore, significantly contribute to the hydrometeorological characterization of watersheds, especially in large and/or inaccessible watersheds where *in situ* collection of environmental data is constrained by resources, feasibility, and infrastructure.

Physical and empirical hydrologic modeling of a watershed's response to a precipitation event depends on the characterization and/or quantification of soil moisture antecedent to the precipitation and subsequent streamflow events. The spatial variability of soil properties and their respective infiltration characteristics suggest that physical approaches can lead to massive data requirements if *in situ* estimations of soil moisture and infiltration dynamics are required across a large watershed. In general, the spatial and temporal status of soil moisture is inadequately characterized in many physical and empirical models.

The objective of this present study is to evaluate and demonstrate how MODIS time series of landscape biophysical variables, as potential proxies of antecedent moisture condition (AMC), may be used to statistically estimate a watershed's streamflow response to precipitation events on an eight-day period, corresponding to relevant MODIS calibrated and validated biophysical products. The primary implication of this research and modeling approach is the generation of generalized flow series for ungauged watersheds (regionally proximate to the calibrated watershed) to facilitate water balance studies and water resource management. The study area is a rural watershed in south-central Texas.

BACKGROUND

The application of remote sensing to the observation of hydrologic state variables has been investigated recently by several authors (Adegoke and

Carleton, 2002; Andersen *et al.*, 2002; Ceccato *et al.*, 2002; Goward *et al.*, 2002; Sandholt *et al.*, 2002; Fensholt and Sandholt, 2003; Zarco-Tejada *et al.*, 2003; Danson and Bowyer, 2004; Weisling *et al.*, 2008). Schmugge *et al.* (2002) summarized the overall contributions of visible, thermal, and passive microwave remote sensing to assessments of key hydrologic states and fluxes such as land surface temperature (LST), surface soil moisture, snow cover, water quality, and evapotranspiration. Reflected solar radiation from the land surface, primarily in the visible to middle infrared (0.4-2.5 μm wavelengths), has been examined for its use in characterizing land use land cover (Green *et al.*, 1994), and for generating hydrologically descriptive vegetation indices (Perry and Lautenschlager, 1984; Huete, 1988; Goward *et al.*, 1991) – both key inputs to hydrologic models. Emitted thermal radiance from the land surface (3.0-14.0 μm wavelengths) can be remotely sensed and quantified as a thermal brightness temperature. If corrected for atmospheric attenuation and surface emissivity, the thermal brightness temperature can be converted to LST. As surface emissivity is partly dependent on moisture content, the LST is coupled directly to surface soil moisture. Microwave radiance (0.15-30 cm wavelengths) is also emitted from the land surface and can be remotely sensed as a microwave brightness temperature. Microwave radiance is strongly influenced by moisture content, because of the large dielectric constant of water (80) compared with <5 for most dry soils. Although this remote sensing technique offers the most direct determination of soil moisture content (Njoku and Kong, 1977; Jackson and Schmugge, 1989; Cashion *et al.*, 2005), the very low spatial resolution (usually >625 km^2 per pixel) renders the method ineffective for the study area in question. It will not be discussed further.

Spectral Vegetation Indices and Soil Moisture

There is an extensive 40+ year history of the development and use of spectral vegetation indices as indicators of biophysical properties of vegetation (Jensen, 2000). Many indices have been specifically developed to function as indicators of plant water content, or water stress such as the Moisture Stress Index (MSI) (Rock *et al.*, 1986), the Leaf Relative Water Content Index (LWCI) (Hunt *et al.*, 1987), the Normalized Difference Water Index (NDWI) (Gao, 1996), the Water Index (WI) (Peñuelas *et al.*, 1997), and the Global Vegetation Moisture Index (GVMI) (Ceccato *et al.*, 2002). Other indices, such as the Normalized Difference Vegetation Index (NDVI) (Rouse *et al.*, 1974) and the Enhanced Vegetation Index (EVI) (Huete and Justice, 1999) were developed as more general

indicators of vegetation biomass, phenology, and net primary productivity. Vegetation is of course coupled physically and biophysically to soil, and so vegetation water content and status is a potential proxy for soil moisture status.

Vegetation as an indirect indicator of soil moisture status at the near surface has been explored by Fensholt and Sandholt (2003) in a study of a semi-arid region of Senegal in 2001 and 2002. Two water stress indices derived from MODIS near infrared (NIR-MODIS band 2) and shortwave infrared (SWIR-MODIS bands 5 and 6) channels correlated well with *in situ* soil moisture sampling at 10 cm at 10 sites ($r^2 = 0.87$ and 0.79). A correlation analysis of root zone soil moisture (at depths ranging from 5 cm to 100 cm) and MODIS NDVI at semi-arid and humid shrub and grassland sites in the southern and southwestern U.S. by Wang *et al.* (2007) demonstrated that deseasoned time series of NDVI significantly correlated with deseasoned root zone soil moisture at all three examined sites. An additional result of this study indicated that vegetation response at all sites lagged root zone soil moisture anomalies by up to 10 days depending on vegetation type and climate. Adegoke and Carleton (2002) examined the correlation of NDVI and neutron probe soil moisture measurements on cropland and forest sites in the Midwestern U.S. The deseasoned time series of NDVI were only weakly correlated with soil moisture though stronger relations were found when a deseasoned composite NDVI (3×3 , 5×5 , etc. pixel composite) was lagged at least two weeks from associated soil moisture anomalies. An association of LST and vegetation canopy water stress was first proposed by Jackson *et al.* (1977) which led to the Crop Water Stress Index (CWSI). This work was further explored by Nemani and Running (1989) in their investigations of surface temperature (T_s) and vegetation stress/soil moisture deficit, known as T_s /NDVI space. Related to stomata resistance and evapotranspiration, the T_s /NDVI relationship has led to the Temperature-Vegetation Dryness Index (TVD). Sandholt *et al.* (2002) have applied the TVD to simulated soil moisture in a distributed hydrologic model based on MIKE SHE code and have found good correlation ($r^2 = 0.70$) in a study of the semi-arid sahel in northern Senegal.

Land Surface Temperature and Soil Moisture

LST is directly coupled to soil moisture through the efficiency of radiant energy transmission between the surface and atmosphere. A portion of incoming shortwave solar radiance, absorbed by the Earth surface, is eventually re-emitted as either longwave infrared radiation and/or microwave radiation. The thermal

emission depends on the physical properties of the surface materials such as composition, surface roughness, and emissivity. The emissivity is a measure of efficiency of radiant energy transfer of a material and is directly affected by moisture content. It is a unitless quantity ranging from 0 to 1 (perfect emitters are blackbodies that emit 100% of absorbed radiant energy). Emitted thermal radiance can ultimately be measured by airborne and satellite radiometers as a brightness temperature of the surface. Once atmospheric attenuation and transmission effects are corrected for, typically through application of radiative transfer codes, knowledge of surface emissivities allow for the derivation of surface temperature from the remotely sensed brightness temperature. Knowledge of the correct emissivity, however, is crucial as a 0.01 difference in emissivity (at a brightness temperature of 300 K) can lead to a 2 K error in LST (Price, 1984).

The moisture content of land surface strongly influences the partitioning of atmosphere energy flux into latent and sensible heat. Through deficits in precipitation, a depletion of soil moisture reduces the rate of evapotranspiration. This in turn forces a re-partitioning of surface heat flux: a decrease in latent heat flux and increase in sensible heat flux. Increased sensible heat flux requires an increase of surface/boundary layer temperature. This physical coupling of LST and surface moisture has been hypothesized to lead to a positive feedback mechanism whereby an induced temperature anomaly from a soil moisture deficit acts to dry the atmosphere and near surface soil. This land-atmosphere feedback has been demonstrated in a study through correlation of soil moisture and temperature anomalies (Durre and Wallace, 2000). In an examination of summertime modeled soil moisture (W) and daily maximum temperature (T_{max}) at 80 stations across the contiguous U.S., they found a dependency of temperature on AMC in the form of a “memory” of soil moisture in the temperature signal (particularly at humid inland stations). As evidence for the moisture – temperature feedback mechanism, they also found higher correlations at both humid inland and arid inland stations when T_{max} led W by 5-10 days rather than lag W .

A streamflow estimation of least squares regression model based on LST, the EVI developed by Huete and Justice (1999) (specifically for improved global vegetation monitoring by the MODIS sensor), and NEXRAD precipitation estimates was developed and compared with streamflow estimates derived from the U.S. Department of Agriculture’s Natural Resource Conservation Service (NRCS) curve number (CN) method for calendar year 2004 (Weissling *et al.*, 2008) in Sandies Creek watershed of south-central Texas. Promising results indicated an improved estimation of eight-day mean streamflow derived from regression analysis of

remotely-sensed biophysicals over that estimated by the CN method.

Overall, the research described above has important implications for the hypothesis of this present study that remotely sensed LST as well as vegetation canopy biophysicals as represented by Vegetation Indices (VIs) are sufficiently coupled to antecedent soil moisture condition to statistically explain a significant proportion of variation of streamflow.

STUDY AREA

The Guadalupe and San Antonio river basins extend from their headwaters on the Edwards pla-

teau in central Texas to the Texas gulf coast estuaries and bays (Figure 1). The middle regions of these basins, as selected for this study, are bounded to the northwest by the Balcones escarpment, and to the southeast by the gently sloping coastal plains. Topographically, these mid-basin watersheds are characterized by low rolling hills and gently sloped stream valleys. Sandies Creek, a tributary of the Guadalupe River, drains approximately 2,000 km of predominately rural land in Guadalupe, Gonzales, Wilson, Karnes, and DeWitt counties. The landscape bounded by the extent of the Sandies Creek watershed is represented by 16 individual land cover classes in eight categories. Four categories – forested land, shrubland, grassland, and pasture/cultivated lands – represented 98.9% of the total land area of the watershed, the remainder being wetlands, urban lands, barren

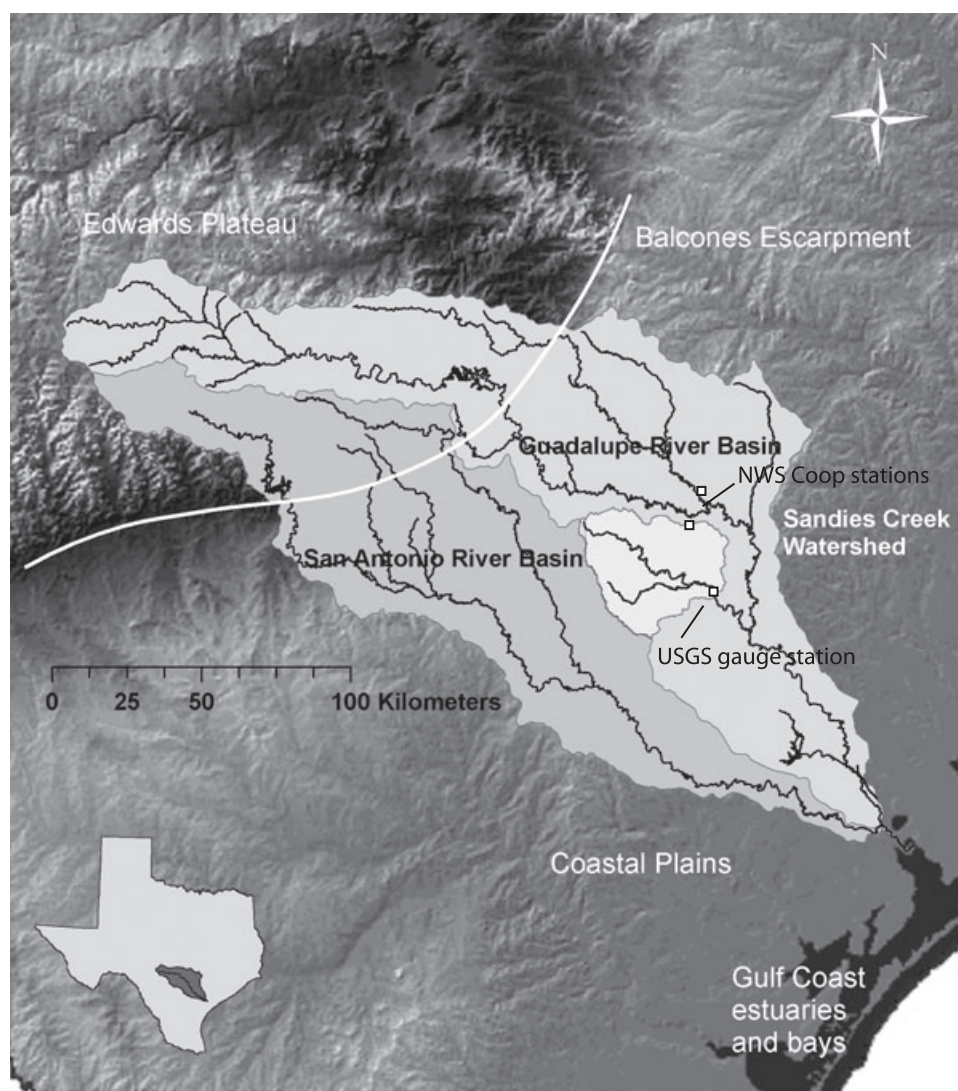


FIGURE 1. Location of Sandies Creek Watershed and the Guadalupe and San Antonio River Basins of South-Central Texas. The river basins straddle the Gulf coastal plains, the Balcones Escarpment, and the Edwards Plateau. Sandies Creek watershed (white) encompasses 1,420 km².

lands, and open water. Soil hydrologic group types were predominately D and C (soil types with low infiltration and high runoff potential), representing 57% and 21% of the total watershed area, respectively. Soil types B and A (soils with higher infiltration but lower runoff potential), represented 13% and 9% of watershed area, respectively.

Precipitation in the region is primarily convective, typically associated with the convergence of frontal systems and moisture masses moving inland from the Gulf of Mexico, as well as from the Gulf of California and Pacific Ocean. Mean annual precipitation across the respective river basins ranges from 750 to 1,050 mm, along a west to east gradient. The majority of significant rainfall events occur in late spring (May-June) and early autumn (September-October). The region is also known for locally intense precipitation events that are attributed to the orographic influence of the Edwards Plateau and Balcones Escarpment, tropical moisture streams from the Gulf of Mexico and/or the Pacific, and the destabilizing influence of late spring and early autumn frontal systems. This region of central Texas holds numerous world records for precipitation intensities, from 2-h events to two-day events (Larkin and Bowmar, 1983; Smith *et al.*, 2000). Likewise, the region is also home to catastrophic flood events. Sandies Creek watershed has an extensive history of agricultural use and the stream course itself has recently been listed, along with neighboring Elm Creek, as an impaired stream by the Texas Commission on Environmental Quality (Texas Commission on Environmental Quality, 2006). The watershed also has a significant history of flooding. An understanding of the watershed's runoff response to precipitation events is therefore critical to developing a water quality assessment and flood mitigation program.

DATA AND PREPROCESSING

Precipitation and Streamflow Data and Preparation

Initial work on this streamflow estimation model was based on gauged rainfall estimates from two National Weather Service (NWS) Cooperative weather stations located near the northeastern boundary of the watershed (Gonzales 10SW and Gonzales 1N). The assumption that two gauged data records would reliably represent spatially varying precipitation within the watershed was questionable. This study utilizes precipitation estimates from the NWS NEXRAD Stage III and Multisensor Precipitation Estimator (MPE) data products. The wide use of

NEXRAD precipitation estimation products in hydro-meteorology and climatology, precipitation, flood, and weather forecasting has been well documented (Johnson *et al.*, 1999; Young *et al.*, 2000; Krajewski and Smith, 2002). Stage III precipitation products represent composites of precipitation rates from multiple weather radars for a River Forecast Center (RFC) and are corrected with multiple surface precipitation gauges (Xie *et al.*, 2006). These products are available from November 1994 to December 2004 for the West Gulf RFC, the RFC encompassing the Sandies Creek study area. Beginning in 2000, the Stage III product was redeveloped to become the MPE product via software algorithm changes, improved bias adjustment and correction, incorporation of satellite precipitation estimates, and improved mosaicing strategies (online reference – http://www.nws.noaa.gov/oh/hrl/dmip/stageiii_info.htm). Both Stage III and MPE hourly precipitation products are provided by the NWS in a 4 × 4 km polar stereographic grid [Hydrologic Rainfall Analysis Project (HRAP) projection] for an entire RFC and are distributed via the internet in compressed binary (XMRG) format monthly files. The conversion of these bundled monthly files to hourly precipitation rates for specific cells within the study watershed involves a multi-step processing effort (Xie *et al.*, 2005). Sandies Creek watershed encompasses 86 4 × 4 km² cells.

Daily precipitation data utilized in this study originated with hourly NEXRAD Stage III data from January 2002 to September 2003 and hourly MPE data from October 2003 through March 2007. A United States Geologic Survey (USGS) streamflow gauge station (ID 8175000) (29.2153 N, 97.4494 W), located upstream from the confluence of Sandies Creek with the Guadalupe River, was selected to delineate a 1,420 km² watershed, using ArcGIS hydrology tools (ESRI, 2002). Hourly precipitation rates for all NEXRAD cells were composited to a daily mean uniform rate for the watershed. Descriptive statistics for both precipitation and streamflow are shown in Table 1. Long-term mean precipitation for the region is 820 mm per year. Overall, 2002 was an anomalous year for the watershed and region with well above average precipitation and two very significant flood events. Year 2003 was drier than normal, 2004 slightly wetter than normal, and 2005 and 2006 represented as drought years, with 2006 accumulating <50% of normal rainfall (Figure 2). Only the first three months of the 2007 data are used for the study, giving a clear indication of a wetter year.

Prior to compositing the daily mean precipitation and streamflow rates to an eight-day simple mean to correspond to the MODIS eight-day composite data products, a Pearson's correlation analysis between daily precipitation and streamflow events for the

TABLE 1. Descriptive Statistics of Daily and Yearly Total Precipitation (P) and Daily Streamflow (Q) for the Period of Analysis.

	2002		2003		2004		2005		2006		2007 ¹	
	P	Q	P	Q	P	Q	P	Q	P	Q	P	Q
Mean	3.84	6.61	1.79	2.20	2.56	3.54	1.37	2.07	1.07	0.15	2.78	6.55
SD	11.54	29.08	5.52	7.46	6.65	11.13	4.64	6.41	3.80	0.38	9.35	22.91
Max	87.06	404.69	49.50	74.99	45.73	121.11	37.44	48.96	37.75	2.91	56.57	180.27
Total	1401.20	208.30	653.70	69.41	937.80	112.10	501.0	65.16	390.90	4.71	250.90	50.97

Notes: Units of precipitation are mm/d and units of streamflow are m^3/s . Total of precipitation is in mm, total of streamflow is in $m^3 \times 10^6$.

¹Only the first three months of data used for 2007.

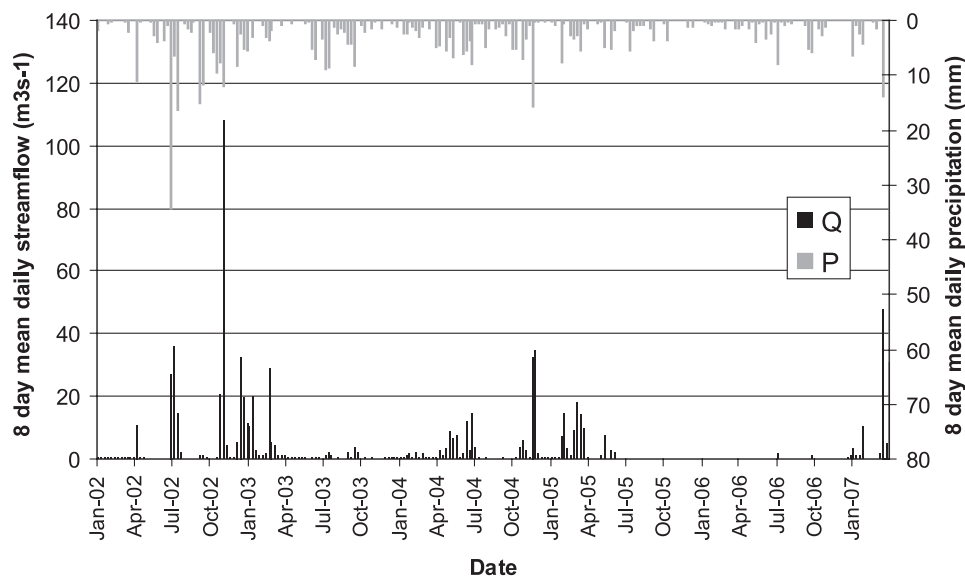


FIGURE 2. Eight-Day Mean Streamflow (m^3/s) at the Outlet of Sandies Creek Watershed (USGS Gauge Station 8175000) and Precipitation (mm) for 2002-2007 (March).

model calibration period (2002-2005) revealed the highest correlation to be associated with daily precipitation events preceding the daily streamflow peaks by three days, a time offset slightly greater than the mean of the lag time of this watershed's streamflow response to significant precipitation events. Shifting the time series by three days, prior to aggregating, is sufficient to ensure that the majority of precipitation events will fall within the same eight-day aggregation period as the ensuing streamflow event. Note that an eight-day data period described as a calendar date (the January 9 temperature event for example) signifies the composited events from January 9 to January 16.

MODIS Biophysical Data and Preparation

Many land surface remote sensing studies demand high spatial and spectral resolution data. However, an assessment of biophysical proxies for

soil moisture condition in a lumped parameter streamflow estimation model is more dependent on high temporal resolution. MODIS on the Terra satellite, launched in 1999, images the entire earth surface every one to two days in 36 spectral bands from the visible to the thermal infrared (<http://modis.gsfc.nasa.gov>). MODIS raw data (Level 1A and 1B) and processed products (Levels 2, 3, and 4) at spatial resolutions ranging from 250 to 1,000 m are processed and delivered at no cost to the public by the Earth Resources Observation Systems (EROS) data center of the USGS. MODIS data products utilized in the study were: the Land Surface Temperature/Emissivity Level 3 (MOD11A2) eight-day (1 km spatial resolution) product, and the Vegetation Indices Level 3 (MOD13A2) 16-day (1 km) product. The MOD11A2 product provides a day and night average surface temperature estimation of the composited vegetation canopy and soil, with an accuracy of 1 degree Kelvin (Wan *et al.*, 2004). The MOD13A2 product provides the standard NDVI, an EVI, and

reflectivity of individual MODIS bands 3 (blue, 0.459-0.479 μm), 1 (red, 0.620-0.670 μm), 2 (near infrared, 0.841-0.876 μm), and 7 (shortwave infrared, 2.105-2.155 μm). These MODIS products are corrected for atmospheric scattering and absorption.

All original MODIS data, in Hierarchical Data Format-Earth Observing System (HDF-EOS) format, were re-projected from the original Equal-Area Sinusoidal projection to a local Universal Transverse Mercator (UTM) (Zone 14, WGS84 datum) projection and then spatially subsetted to the bounding coordinates of the study area in a new GeoTIFF image format. This was accomplished using a software tool called the MODIS Re-Project Tool, ~available from the USGS web portal online at <http://edcdaac.usgs.gov/datatools.asp>. An ArcInfo Arc Macro Language (AML) script (Xie *et al.*, 2005; Zhou *et al.*, 2005) was employed to convert the subsetted MODIS TIFF images to an ArcGIS grid format, to clip each grid by the polygon coverage of the watershed boundary, and to create ASCII text output of all pixel values. These pixel values represented eight-day means for the LST products and 16-day means for the vegetation products. An eight-day interpolated vegetation product was generated from the 16-day product by assigning the second half of a 16-day period (as the new eight-day step) to the simple mean of two adjacent 16-day values. The authors assert that this technique (essentially a smoothing operation) is valid for vegetation biophysical given the gradual nature of vegetation change. Finally, all MODIS pixel values for a given eight-day timestep were then composited (as a simple mean) for the watershed.

All time series were quality controlled for bad data points. Because of the greater likelihood of an eight-day composited image suffering from cloud cover, the eight-day LST products had considerably more quality issues than the 16-day products. Any eight-day period or time step with >75% “no data” pixels (1,428 total pixels in the watershed) was discarded. In a few isolated cases, an eight-day time step would pass the “no data” quality control test, but would clearly be an anomaly compared with the before and after time steps. These anomalies would typically be represented by large positive or negative spikes in the temperature products and were discarded (10 of the total 184 time steps for the study period).

Vegetation Indices and Development

Normalized Difference Vegetation Index. NDVI is defined as the normalized ratio of the near-infrared reflectance response of a surface to the red response.

With vegetation, the red response is located in the strong chlorophyll absorption region, while the infrared response is located on the high reflectance plateau of the near infrared. For MODIS, NDVI is calculated as:

$$\text{NDVI} = \frac{R_{\text{nir}} - R_{\text{red}}}{R_{\text{nir}} + R_{\text{red}}}, \quad (1)$$

where R_{nir} is the reflectance response at band 2, and R_{red} is the reflectance response at band 1. NDVI responds most directly to vegetation activity (photosynthesis), biomass, and chlorophyll levels, but also indirectly to canopy density and soil moisture induced vegetation stress.

Enhanced Vegetation Index. EVI is a modified NDVI developed specifically for MODIS data (Huete and Justice, 1999). EVI has improved sensitivity to high biomass regions and is de-sensitized to canopy background signal and atmospheric influences (Gao *et al.*, 2000; Miura *et al.*, 2001). EVI is calculated as:

$$\text{EVI} = \frac{\rho_{\text{nir}} - \rho_{\text{red}}}{\rho_{\text{nir}} + C_1\rho_{\text{red}} - C_2\rho_{\text{blue}} + L}(1 + L), \quad (2)$$

where ρ is band reflectance precorrected for atmospheric scattering. The coefficients C_1 , C_2 , and L are empirically determined as 6.0, 7.5, and 1.0, respectively.

Moisture Stress Index. MSI is a vegetation index sensitive to moisture stress. It was originally developed by Rock *et al.* (1986) based on the Landsat Thematic Mapper near infrared (NIR) band 4 and middle infrared (MidIR) band 5. Band 4 for Landsat TM, centered at wavelength 0.83 μm , is quite insensitive to moisture change in vegetation while band 5, at wavelength 1.65 μm , responds dramatically to moisture change in vegetation. MSI is calculated as:

$$\text{MSI} = \frac{\text{MidIR}}{\text{NIR}} \quad (3)$$

The MSI index utilized in this study is a modified version based on another region of the middle infrared, the wavelength channel centered at 2.10 μm , MODIS band 7. Band 7 is also dominated by vegetation water absorption and is thus sensitive to variations of vegetation water content (Chen *et al.*, 2005).

Normalized Difference Water Index. NDWI is a normalized water stress index based on the same

wavelength channels as MSI (Gao, 1996). It is defined as:

$$\text{NDWI} = \frac{R_{\text{nir}} - R_{\text{swir}}}{R_{\text{nir}} + R_{\text{swir}}}, \quad (4)$$

where R_{swir} is the reflectance in a shortwave (also referred to as MidIR) infrared channel (1.2-2.5 μm). For this study, MODIS band 7 at 2.1 μm was used.

Time Series Development. Theoretically, the seasonal component of a time series can lead to covariance issues and subsequent inflation of model significance in a regression or correlation analysis. Deseasoned time series of precipitation and soil moisture are evaluated in a recent study (Wang *et al.*, 2007). The seasonal time series in this model was first calculated by averaging the eight-day raw time series (2002 through 2005) followed by a 3-point smoothing of the means. The four-year smoothed mean time series were then subtracted from the annual time series to obtain a deseasoned time series.

$$\text{TS}_{\text{ds}} = \text{TS}_{\text{raw}} - \text{TS}_{\text{sm}} \quad (5)$$

$$\text{TS}_{\text{sm}} = \left(\frac{\sum_{j=t-1}^{t+1} \sum_{i=1}^n \text{TS}_{\text{raw}}}{n} \right) / 3, \quad (6)$$

where TS_{ds} is the eight-day deseasoned mean in a time series, TS_{raw} is the eight-day raw mean in a time series, TS_{sm} is the 3-point smoothed eight-day mean in a time series, n represents the number of years for which the deseasoned time series is computed, and j represents the value immediately before and after an event value at time t .

Both raw and deseasoned time series for the two temperature products (LSTday, LSTnight), two vegetation indices (NDVI, EVI), two individual reflectance bands (MODIS bands 2 and 7), and two user-derived moisture stress indices (MSI, NDWI) were produced (Figure 3). Table 2 shows the minimum and maximum values of all parameters used in the study.

While long-term means are considered appropriate for deseasonalizing time series, the limited availability of MODIS products necessitated the use of only four data years to calculate the mean. Each time series was then advanced by one and two 8-day periods to test for antecedent effects. All together, 16 individual remote sensing-based parameters were

produced and evaluated in the model: eight raw series and eight deseasoned series with time offsets of 0, 8, and 16 days. This generated 48 individual parameters together with precipitation ($n = 49$) to be evaluated in the forward stepwise regression parameter selection.

All time offsets (as multiples of eight-day periods) are denoted as subscripts to the parameter names listed above, as in $\text{LSTd}_{r(2)}$ to denote a two period (or 16 days offset) of daytime LST raw product (hereafter).

STATISTICAL MODEL DEVELOPMENT AND EVALUATION

Prior to performing the forward stepwise regressions, a distribution analysis of the eight-day mean gauged streamflow record indicated a non-normal distribution of events, verified by the Shapiro-Wilks statistical test for normality. A log transformation of the streamflow data satisfied the normal distribution assumptions for least squares regression models.

The large number of parameters to be evaluated ($n = 49$) necessitated selecting the “best” parameter subset for inclusion in the least-squared regression model. Forward stepwise regression is a data mining method to evaluate the significance of a parameter in reducing the sequential sum of squares of the model as that parameter enters the model. The significance probability criteria for entering the model was set at $p = 0.10$. The first parameters to enter the model are generally the most significant and will explain the greatest proportion of variation of the dependent variable, streamflow in this case. A measure of the goodness of fit of multiple regression models is the Mallows Cp criteria; when the value of Cp approaches the number of parameters that have entered the model, the model is interpreted to be properly fit. Although a number of parameters may be retained in the forward selection process, only those that significantly contribute to the overall coefficient of determination, r^2 , and are not collinear to other parameters [such as $\text{EVI}_{\text{ds}(1)}$ and $\text{EVI}_{\text{ds}(2)}$], are included in the final least-squares model.

The evaluation of the regression model is based on the coefficient of determination adjusted for multiple regressors (r^2_{adj}) while the final calibration and validation model performance is based on the Nash-Sutcliffe estimation efficiency (E) for log-transformed flow series, and the relative volume error or bias (B).

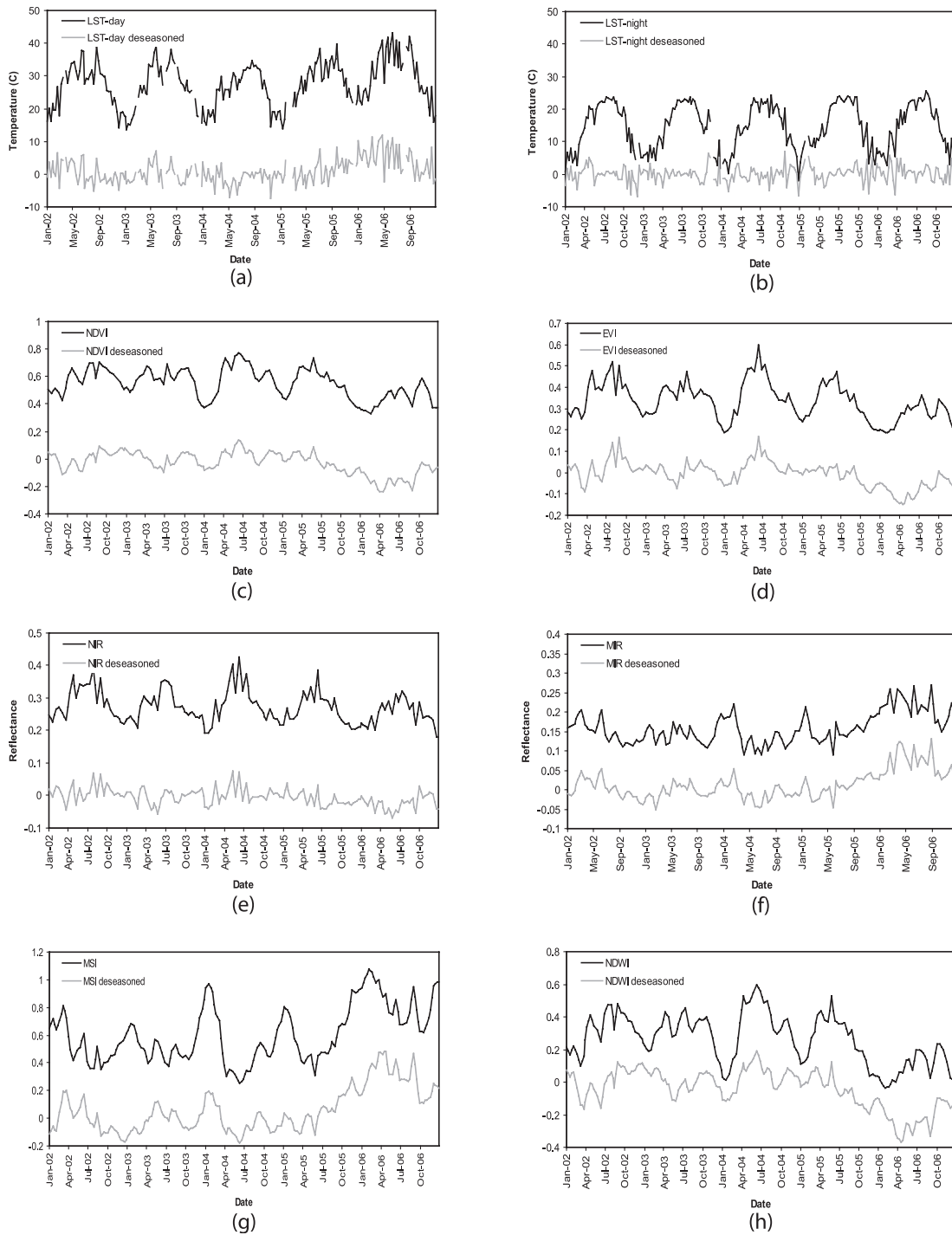


FIGURE 3. Raw and Deseasoned Time Series Plots for Eight-Day Time Steps, 2002-2007 (March). (a) Daytime land surface temperature, (b) nighttime land surface temperature, (c) normalized difference vegetation index, (d) enhanced vegetation index, (e) NIR reflectance, (f) MIR reflectance, (g) moisture stress index, (h) normalized difference water index. NDVI, EVI, MSI, and NDWI are unitless ratios.

The Nash-Sutcliffe efficiency (E) criterion is a common efficiency criterion applied to performance of hydrologic models, originally developed by Nash and Sutcliffe (1970) for river flow forecasting models. It is calculated as:

$$E = 1 - \left(\frac{\sum_{i=1}^n (O_i - PV_i)^2}{\sum_{i=1}^n (O_i - \bar{O})^2} \right), \quad (7)$$

TABLE 2. MODIS Remote Sensing Parameters Evaluated in This Study.

Name	Full Name	Range	
		Minimum	Maximum
LSTd_r	Daytime land surface temperature (raw)	13.70	39.70
LSTd_ds	Daytime land surface temperature (deseasoned)	-7.60	8.30
LSTn_r	Nighttime land surface temperature (raw)	-2.0	24.20
LSTn_ds	Nighttime land surface temperature (deseasoned)	-7.0	7.0
NDVI_r	Normalized Difference Vegetation Index (raw)	0.37	0.77
NDVI_ds	Normalized Difference Vegetation Index (deseasoned)	-0.13	0.14
EVI_r	Enhanced Vegetation Index (raw)	0.19	0.60
EVI_ds	Enhanced Vegetation Index (deseasoned)	-0.09	0.17
NIR_rs	Near-infrared radiance (MODIS band 2) (raw)	0.19	0.43
NIR_ds	Near infrared radiance (MODIS band 2) (deseasoned)	-0.06	0.08
SWIR_r	Shortwave infrared radiance (MODIS band 7) (raw)	0.09	0.22
SWIR_ds	Shortwave infrared radiance (MODIS band 7) (deseasoned)	-0.05	0.05
MSI_r	Moisture Stress Index (raw)	0.25	0.97
MSI_ds	Moisture Stress Index (deseasoned)	-0.18	0.29
NDWI_r	Normalized Difference Water Index (raw)	0.01	0.59
NDWI_ds	Normalized Difference Water Index (deseasoned)	-0.20	0.19

with O_i being observed and PV_i being predicted values.

The range of E lies between 1 (for a perfect fit) and $-\infty$. An E value lower than zero indicates that the mean of the observed time series would likely have been a better predictor than the model. E indicates the degree to which the plot of observed *vs.* modeled values fit the 1:1 line. However, a significant disadvantage of the E criterion is that the squared values of observed and predicted lead to overestimating extreme values in a time series, such as flood events, and neglecting small values such as base flow (Krause *et al.*, 2005). Krause proposes that applying E to log-transformed flow values will reduce the problem of extreme value sensitivity while increasing the influence of low flow values.

The second efficiency criterion to be applied is the relative volume error or bias (B). It is calculated as:

$$B = \frac{\sum_{i=1}^n (PV_i - O_i)}{\sum_{i=1}^n O_i} \quad (8)$$

This efficiency criterion measures the tendency of the modeled values to be smaller or larger than the associated observed values and is typically expressed as a percentage of under or overestimation.

RESULTS

The model is developed and calibrated on 174 time steps for years 2002 through 2005, and validated on

57 time steps covering 2006 and the first three months of 2007.

Forward stepwise regression was performed on 49 regressors, 48 remote sensing parameters and precipitation (P), to determine the optimal subset of parameters for a streamflow estimation regression model. The first three parameters to enter the model [P , LSTd_r(2), and MSI_ds(0)] accounted for 69.6% of the variation of log-transformed streamflow. Three additional parameters [LSTn_r(1), MSI_r(0), and LSTd_r(0)] successfully entered the model, explaining an additional 5.2% of the variation of streamflow (Table 3), but were excluded due to collinearity.

Precipitation accounted for 35.7% of streamflow variation. The second parameter to enter was LSTd_r(2) explaining an additional 23.5% variation. MSI_ds(0) was the third parameter to enter, explaining an additional 10.5% of variation. These three regressors were entered into the least squares regression model, as described by the following generalized equation.

$$\text{Est}(\log Y) = \beta_0 + \beta_1 x_1 + \beta_2 x_2 + \beta_3 x_3, \quad (9)$$

where $\text{Est}(\log Y)$ is the estimate of log-transformed model response, X_i are the predictor variables or regressors, and β_i are the parameter estimates.

The goodness of fit of the least squares regression model, adjusted for multiple regressors (r^2_{adj}), was 0.67. All parameter estimates and the intercept (β_0) were significant at $p < 0.0001$.

The final estimation equation for the calibrated streamflow model was:

TABLE 3. Step History of Forward Stepwise Regression of 49 Parameters for 174 Events, 2002 Through 2005.

Step	Parameter	Action	Significance Probability	Sequential Sum of Squares	r ² Criteria	Mallows Cp Criteria
1	<i>P</i>	Entered	0.0000	192.86	0.3572	232.36
2	LSTd _{r(2)}	Entered	0.0000	126.88	0.5922	93.48
3	MSI _{ds(0)}	Entered	0.0000	56.13	0.6961	33.16
4	LSTn _{r(1)}	Entered	0.0007	12.01	0.7184	21.82
5	MSI _{r(0)}	Entered	0.0006	11.57	0.7398	10.97
6	LSTd _{r(0)}	Entered	0.0271	4.51	0.7482	7.96

$$\log Q = 1.978 + 0.293P - 0.120T - 6.174I, \quad (10)$$

where *Q* is eight-day composited daily mean streamflow in m³/s, *P* is eight-day composited daily mean precipitation in mm (advanced three days prior to compositing), *T* is eight-day composited mean LSTd_{r(2)} in °C, and *I* is eight-day composited mean MSI_{ds(0)}.

The estimation efficiency for the calibrated log-space flow series (January 2002-December 2005, *n* = 174) was 0.68, with efficiencies ranging from 0.48 to 0.79 for individual years (Table 4). Overall bias for the calibrated flow series was 21%. This overestimate of gauged flow was found to be largely dependent on a single extreme flood event in July 2002. If considered to be an outlier, removal of the time step associated with this event resulted in an overall bias of -47%. Bias for individual years in the calibration period are listed in Table 4.

Model validation encompassed 57 time steps corresponding to eight-day records from January 2006 through March 2007. *E* for the complete log-space flow series was 0.45. The bias for the complete flow series was -32% (Table 4). Figures 4 and 5 illustrate the time series of log-space modeled and gauged streamflow for the calibration and validation periods, respectively. Figure 6 illustrates the time series of linear-space modeled and gauged streamflow for the validation period.

DISCUSSION

The calibration phase of the model development yielded a reasonable fit of modeled to gauged streamflow with an *r*²_{adj} of 0.67 and an estimation efficiency of 0.68. The overall level of bias in the calibration series, at 21%, was heavily influenced by the July 2002 event. A 10-fold overestimate of gauged streamflow for that event indicates the nonlinearity of the model for extreme events. A parameter sensitivity test associated with this event indicated that a 27% reduction in aggregated precipitation for the time step was suffi-

TABLE 4. Model Performance Criteria for Log-Space Flow Series for Calibration Period January 2002-December 2005, and for Validation Period January 2006-March 2007.

Model Period	<i>E</i> log Series	Bias
Calibration All (<i>n</i> = 174)	0.677	0.207 (-0.471) ¹
2002 (<i>n</i> = 43)	0.616	1.037 (-0.399) ¹
2003 (<i>n</i> = 42)	0.477	-0.467
2004 (<i>n</i> = 45)	0.705	-0.516
2005 (<i>n</i> = 44)	0.785	-0.627
Validation All (<i>n</i> = 57)	0.453	-0.322
2006 (<i>n</i> = 46)	-0.028	-0.593
2007 (<i>n</i> = 11)	0.871	-0.293

¹Bias values marked denote exclusion of July 2002 flood event.

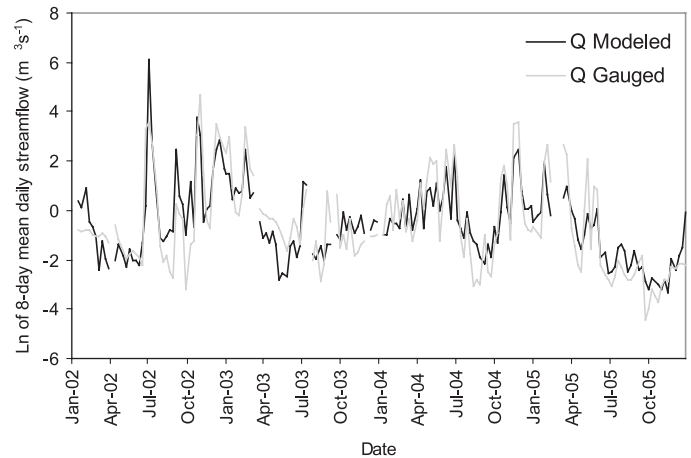


FIGURE 4. Time Series of Log-Space Modeled and Gauged Streamflow for Calibration Period, 2002-2005.

cient to accurately model the gauged flow. The resulting calibration series bias with the July 2002 event excluded, at -47%, indicates the influential role of that outlier in the original regression. In general, the MODIS-derived daytime LST and the user-derived (from MODIS spectral bands) MSI, together accounted for 34% of the variability of streamflow during the four-year calibration period. One must conclude then that these two biophysical parameters are to some significant degree sensitive to the temporal flux of the soil moisture condition in this test watershed.

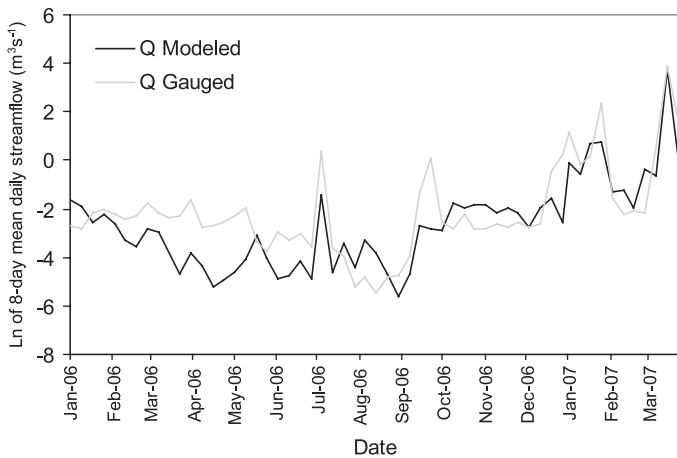


FIGURE 5. Time Series of Log-Space Modeled and Gauged Streamflow for Validation Period, 2006-2007 (March).

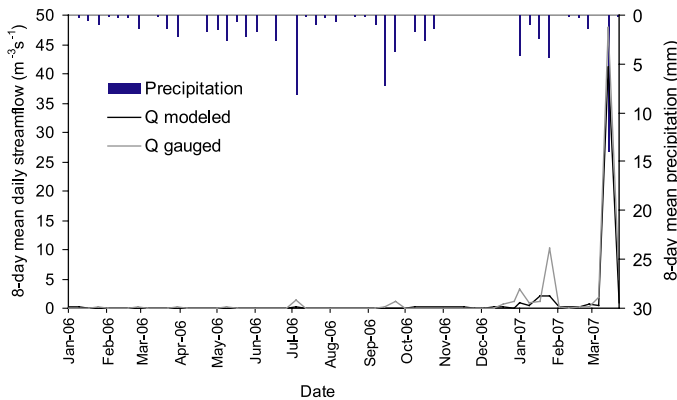


FIGURE 6. Time Series of Linear-Space Modeled and Gauged Streamflow for Validation Period, 2006-2007 (March).

The application of the streamflow estimation equation (Equation 10) to the 57 time steps (as eight-day records) of precipitation, LST, and MSI during the 15-month validation period resulted in reasonable results in the prediction of streamflow. The breakdown of E values for the complete log-transformed series ($E = 0.45$) to the 2006 events ($E = -0.03$) and to the 2007 events ($E = 0.87$) deserves further discussion. With drought conditions predominating during 2006, this model reliably predicted that there would be little if any runoff response to precipitation events when they occurred. However, as the E criteria for 2006 suggests, this model did not reliably predict base-flow levels. Hydrologic conditions outside the scope of the model design, such as ground-water flow, streamflow diversion, etc., would have likely impacted base-flow levels. The performance of the model for flow series during normal to high precipitation conditions in 2007 (first three months) was substantially better ($E = 0.87$), and as such would have

to be considered a reasonably good result. In linear space, rather than in log-space, E is overly sensitive to high flow events and correspondingly insensitive to low flow events and to systematic underprediction or overprediction or bias (Krause *et al.*, 2005). Krause suggested that the E criterion applied to log-transformed flow series will result in improved influence of the low flow events in model performance as well as greater sensitivity to bias.

Overall, the model underestimated streamflow for the wet period from January 1 to March 30, 2007 by 29.4%, with mean gauged daily streamflow at $6.40 \text{ m}^3/\text{s}$ and mean modeled daily streamflow at $4.62 \text{ m}^3/\text{s}$. Precipitation during the period from January 1, 2006 to December 27, 2006 was approximately 50% of the long-term mean, close to the drought of record that occurred during the 1950s. Mean modeled streamflow for this 2006 drought period was $0.066 \text{ m}^3/\text{s}$ vs. mean gauged streamflow of $0.14 \text{ m}^3/\text{s}$, an underestimate of 59.3%. The model underestimation for the validation period (all 15 months) was 32.2% as indicated earlier by the bias criteria.

Approximately 60% of the variability of log-space gauged streamflow in the validation series was explained by the model, leaving 40% of the variability unaccounted for. The latter is sufficient to explain the rather unimpressive performance of the model as assessed by the estimation efficiency (0.45). However, given that the efficiency was assessed in log-space, subjective evaluation of what this indicates is left up to the reader. The remaining variance in the overall model was randomly distributed about the mean, as was demonstrated by a plot of model residuals (not shown). Multiple sources of uncertainty in the model parameters as well as known sources of error in model design likely explain model discrepancies and model bias. Known sources of model discrepancy include the unavoidable time-step separation of some precipitation events from their corresponding streamflow events. Compositing distributed parameter values over such a large watershed area no doubt introduces significant uncertainty and discrepancy. LST and MSI anomalies in a large watershed might not be spatially associated with a significant precipitation event – spatial associations necessarily lost in the compositing process. One potential source of model discrepancy is the error induced by the creation of the interpolated eight-day MSI time series from the 16-day original vegetation index product. Unlike LST, there is no quantification of uncertainty for the MSI time series itself as there is no physical meaning to the MSI (or to any vegetation index). For the MODIS LST product, there is a published uncertainty of ± 1 degree K (Wan *et al.*, 2004). An analysis of the sensitivity of the model to an error in LST of 1 degree (-1 degree because of the negative correlation

of LST with Q), resulted in an improvement in the bias for the overall validation period from 32% to 22%. Rather than systematic error, random LST uncertainties of ± 1 degree K applied to individual time steps could explain some remaining variance in the final model. An analysis of the sensitivity of the model to precipitation uncertainties indicates that a mean increase in precipitation of 11% is sufficient to account for the 32% underestimation in modeled streamflow. This level of NEXRAD uncertainty is certainly possible and is well documented (Young *et al.*, 2000; Jayakrishnan *et al.*, 2004). Young *et al.* (2000) found a 20% underestimate bias in Stage III products in a 5.5-year study from the Arkansas-Red River Basin River Forecast Center. This study also indicated that Stage III products registered significantly fewer precipitation hours than gauged observations of light precipitation. In a similar time frame of the Young study (late 1990s), Jayakrishnan *et al.* (2004) found a general underestimate bias of Stage III precipitation at 545 weather stations covering the Texas-Gulf basin. Estimation bias at First Order/FAA weather stations ($n = 24$) during the five-year study ranged from -2% to -50%. Nash-Sutcliffe estimation efficiencies for these same stations ranged from 0.92 to -0.32. The station in the study most proximate to Sandies Creek watershed, San Antonio International Airport, had the highest E efficiency, 0.92, with an estimation bias of -9% for the five-year period. A more recent study by Wang *et al.* (2008) of Stage III and MPE radar and gauged precipitation in the upper Guadalupe River basin (Sandies Creek watershed is within this basin) contradicted the Young and Jayakrishnan studies in part, in that Stage III radar overestimated gauged precipitation by 19.5% for 2001. MPE radar, however, underestimated gauged precipitation in 2004 by 7.2%. It is recognized that a systematic linear bias in model parameters will be removed from the model during regression, and thus would not account for overall model bias. It is clear, however, that the bias estimates described in these recent NEXRAD studies is nonsystematic. Estimation bias for large precipitation events will have a significantly greater influence on this model's results than bias for small events

CONCLUSION

Four years of MODIS time series imagery of biophysical states of the landscape and NEXRAD multi-sensor precipitation estimation products were assessed for their ability to statistically predict an eight-day mean streamflow response to eight-day

mean precipitation events in a south-central Texas watershed. Sixteen primary raw and deseasoned remote sensing-derived parameters (and 32 variants of those parameters offset in time), hypothesized to be sensitive to or indicative of AMC, were assessed for statistical significance in a forward stepwise regression. Three parameters were selected from the stepwise regression for inclusion in the final least squares regression: NEXRAD precipitation, MODIS daytime LST (16 days antecedent to the streamflow event), and a deseasoned indice of land surface moisture stress. The latter indice was derived from MODIS infrared bands 2 and 7. The prediction equation, calibrated for the period 2002-2005, was validated for the 15-month period January 2006 through March 2007. Model performance was assessed with the Nash-Sutcliffe estimation efficiency applied to the log-transformed flow series ($E = 0.45$). E was also determined for both the log-transformed 2006 flow series (drought conditions) ($E = -0.03$) and the 2007 flow series (wet conditions) ($E = 0.87$). A second performance criterion, the estimation bias, at -0.32, indicated a cumulative underestimation of observed flow. Levels of uncertainty in the MODIS temperature product and in the NEXRAD precipitation products were explored for their potential to account for the underestimation bias and overall model discrepancy. From this study, it is suggested that time series satellite imagery holds significant promise for analysis of the role of landscape moisture status in the subsequent modeling of a watershed's streamflow response to precipitation events. Future research in watersheds of varying spatial dimension under similar and differing environmental and climatological conditions is anticipated for validation of this streamflow modeling concept.

ACKNOWLEDGMENTS

The study was partly supported by a graduate fellowship of the Texas Space Grant Consortium and the Environmental Science and Engineering PhD scholarship at University of Texas at San Antonio to the first author, and a U.S. Department of Education grant (#P120A050061) and a NASA grant (#NNX07AL79G) to the second author. Special thanks to Richard French and Hatim Sharif for their assistance in reviewing the original manuscript. Data provided by NASA, USGS, NOAA/NWS, and Greg Story are sincerely acknowledged. The first author would also thank Keying Ye for his advice on the development of the statistical model, and special thanks to his colleagues at SWCA, Inc. for their support and encouragement.

LITERATURE CITED

- Adegoke, J. and A.M. Carleton, 2002. Relations Between Soil Moisture and Satellite Vegetation Indices in the U.S. Corn Belt. *Journal of Hydrometeorology*, 3(4):395-405.

- Ajami, N.K., H. Gupta, T. Wagener, and S. Sorooshian, 2004. Calibration of a Semi-Distributed Hydrologic Model for Streamflow Estimation Along a River System. *Journal of Hydrology*, 298:112-135.
- Andersen, J., G. Dybkjaer, K.H. Jensen, J.C. Refsgaard, and K. Rasmussen, 2002. Use of Remotely Sensed Precipitation and Leaf Area Index in a Distributed Hydrologic Model. *Journal of Hydrology*, 264:34-50.
- Bedient, P.B., A. Holder, J.A. Benevides, and B.E. Vieux, 2004. Radar-Based Flood Warning System Applied to Tropical Storm Allison. *Journal of Hydrologic Engineering*, 8(6):308-318.
- Carpenter, T.M., K.P. Georgakakos, and J.A. Sperflage, 2001. On the Parametric and NEXRAD-Radar Sensitivities of a Distributed Hydrologic Model Suitable for Operational Use. *Journal of Hydrology*, 253:169-193.
- Cashion, J., V. Lakshmi, D. Bosch, and T.J. Jackson, 2005. Microwave Remote Sensing of Soil Moisture: Evaluation of the TRMM Microwave Imager (TMI) Satellite for the Little River Watershed, Tifton, Georgia. *Journal of Hydrology*, 307:242-253.
- Ceccato, P., N. Gobron, S. Flasse, B. Pinty, and S. Tarantola, 2002. Designing a Spectral Index to Estimate Vegetation Water Content From Remote Sensing Data: Part 1 Theoretical Approach. *Remote Sensing of Environment*, 82:188-197.
- Chen, D., J. Huang, and T.J. Jackson, 2005. Vegetation Water Content Estimation for Corn and Soybeans Using Spectral Indices From MODIS Near- and Short-Wave Infrared Bands. *Remote Sensing of Environment*, 98:225-236.
- Danson, F.M. and P. Bowyer, 2004. Estimating Live Fuel Moisture Content From Remotely Sensed Reflectance. *Remote Sensing of Environment*, 92:309-321.
- Durre, I. and J.M. Wallace, 2000. Dependence of Extreme Daily Maximum Temperatures in Antecedent Soil Moisture in the Contiguous United States During Summer. *Journal of Climate*, 1:2641-2651.
- ESRI, 2002. ArcHydro: GIS for Water Resources. Environmental Systems Research Institute, Inc., Redlands, California.
- Fensholt, R. and I. Sandholt, 2003. Derivation of a Shortwave Infrared Water Stress Index From MODIS Near- and Shortwave Infrared Data in a Semiarid Environment. *Remote Sensing of Environment*, 87:111-121.
- Gao, B.C., 1996. NDWI – A Normalized Difference Water Index for Remote Sensing of Vegetation Liquid Water From Space. *Remote Sensing of Environment*, 58:257-266.
- Gao, X., A.R. Huete, W. Ni, and T. Miura, 2000. Optical-Biophysical Relationships of Vegetation Spectra Without Background Contamination. *Remote Sensing of Environment* 74:609-620.
- Goward, S.N., B. Markham, D.G. Dye, W. Dulaney, and J. Yang, 1991. Normalized Difference Vegetation Index Measurements From the Advanced Very High Resolution Radiometer. *Remote Sensing of Environment*, 35:257-277.
- Goward, S.N., Y. Xue, and K. Czajkowski, 2002. Evaluating Land Surface Moisture Conditions From the Remotely Sensed Temperature/Vegetation Index Measurements – An Exploration With the Simplified Biosphere Model. *Remote Sensing of Environment*, 79:225-242.
- Green, K., D. Kempka, and L. Lackey, 1994. Using Remote Sensing to Detect and Monitor Land-Cover and Land-Use Change. *Photogrammetric Engineering and Remote Sensing*, 60:331-337.
- Huete, A.R., 1988. A Soil-Adjusted Vegetation Index (SAVI). *Remote Sensing of Environment*, 25:295-309.
- Huete, A.R. and C. Justice, 1999. MODIS Vegetation Index (MOD13) Algorithm Theoretical Basis Document. NASA Goddard Space Flight Center, Greenbelt. 129 p.
- Hunt, E.R., B.N. Rock, and P. Nobel, 1987. Measurement of Leaf Relative Water Content by Infrared Reflectance. *Remote Sensing of Environment*, 22:429-435.
- Jackson, R.D., S.B. Idso, and R.J. Reginato, 1977. Wheat Canopy Temperature: A Practical Guide for Evaluating Water Requirements. *Water Resources Research*, 13:651-656.
- Jackson, T.J. and T. Schmugge, 1989. Passive Microwave Remote Sensing System for Soil Moisture: Some Supporting Research. *IEEE Transactions on Geoscience and Remote Sensing*, 27:225-235.
- Jayakrishnan, R., R. Srinivasan, and J. Arnold, 2004. Comparison of Rainage and WSR-88D Stage III Precipitation Data Over the Texas-Gulf Basin. *Journal of Hydrology*, 292:135-152.
- Jensen, J.R., 2000. *Remote Sensing of the Environment: An Earth Resource Perspective*, Prentice Hall, New Jersey, 544 p.
- Johnson, D., M. Smith, V. Koren, and B. Finnerty, 1999. Comparing Mean Areal Precipitation Estimates From NEXRAD and Rain Gauge Networks. *Journal Hydrologic Engineering*, 4(2):117-124.
- Kalinga, O.A. and T. Gan, 2006. Semi-Distributed Modeling of Basin Hydrology With Radar and Gauged Precipitation. *Hydrological Processes*, 20(17):3725-3746.
- Krajewski, W.F. and J. Smith, 2002. Radar Hydrology: Rainfall Estimation. *Advances in Water Resources*, 25:1387-1394.
- Krause, P., D.P. Boyle, and F. Bäse, 2005. Comparison of Different Efficiency Criteria for Hydrologic Models. *Advances in Geoscience*, 5:89-97.
- Larkin, T.J. and G. Bowmar, 1983. *Climatic Atlas of Texas*, Texas Department of Water Resources, LP-192, Austin, Texas, 151 pp.
- Makkeasorn, A., N.B. Chang, and X. Zhou, 2008. Short-Term Streamflow Forecasting With Global Climate Change Implications – A Comparative Study Between Genetic Programming and Neural Network Models. *Journal of Hydrology*, 352:336-354.
- Miura, T., A.R. Huete, H. Yoshioka, and B. Holben, 2001. An Error and Sensitivity Analysis of Atmospheric Resistant Vegetation Indices Derived From Dark Target-Based Atmospheric Correction. *Remote Sensing of Environment*, 78:284-298.
- Moon, J., R. Srinivasan, and J. Jacobs, 2004. Stream Flow Estimation Using Spatially Distributed Rainfall in the Trinity River Basin, Texas, *Transact. ASAE*, 47(5):1445-1451.
- Nash, I.E. and I. Sutcliffe, 1970. River Flow Forecasting Through Conceptual Models. *International Journal of Hydrology* 10:282-290.
- Nemani, R.R. and S.W. Running, 1989. Estimation of Regional Surface Resistance to Evapotranspiration From NDVI and Thermal-IR AVHRR Data. *Journal of Applied Meteorology and Climatology*, 28:276-284.
- Njoku, E.G. and J. Kong, 1977. Theory for Passive Microwave Remote Sensing of Near-Surface Soil Moisture. *Journal of Geophysical Research*, 82:3108-3118.
- Peñuelas, J., R.O. Pinol, R. Ogaya, and I. Filella, 1997. Estimation of Plant Water Concentration by the Reflectance Water Index WI (R900/R970). *International Journal of Remote Sensing*, 18:2869-2875.
- Perry, C.R. and L. Lautenschlager, 1984. Functional Equivalence of Spectral Vegetation Indices. *Remote Sensing of Environment*, 14:169-182.
- Price, J.C., 1984. Land Surface Temperature Measurements From the Split Window Bands of the NOAA 7 Advanced Very High Resolution Radiometer. *Journal of Geophysical Research*, 89:7231-7237.
- Rock, B.N., J.E. Vogelmann, D.L. Williams, A.F. Vogelmann, and T. Hoshizaki, 1986. Remote Detection of Forest Damage. *BioScience*, 36:439-445.
- Rouse, J.W., R.H. Haas, J.A. Schell, and S. Deering, 1974. Monitoring Vegetation Systems in the Great Plains With ERTS. *Proceedings, Third Earth Resources Technology Satellite Symposium*. Greenbelt: NASA SOP-351, 3010-3317.

- Sandholt, I., K. Rasmussen, and J. Andersen, 2002. A Simple Interpretation of the Surface Temperature/Vegetation Index Space for Assessment of Surface Moisture Status. *Remote Sensing of Environment*, 79:213-224.
- Schmugge, T.J., W.P. Kustas, J.C. Ritchie, T.J. Jackson, and A. Rango, 2002. *Remote Sensing in Hydrology*. *Advances in Water Resources*, 25:1367-1385.
- Segond, M., H.S. Wheeler, and C. Onof, 2007. The Significance of Spatial Rainfall Representation for Flood Runoff Estimation: A Numerical Evaluation Based on the Lee Catchment UK. *Journal of Hydrology*, 347:116-131.
- Smith, J.A., M.L. Baeck, J.E. Morrison, and P. Sturdevant-Rees, 2000. Catastrophic Rainfall and Flooding in Texas. *Journal of Hydrometeorology*, American Meteorological Society, 1:5-25.
- Texas Commission on Environmental Quality 2006. Improving Water Quality in Southcentral Texas: Four TMDLs for Bacteria and Dissolved Oxygen in Elm and Sandies Creeks, <http://www.tceq.state.tx.us/assets/public/implementation/water/tmdl/31-elmsandies.pdf>.
- Wan, Z., Y. Zhang, Q. Zhang, and Z. Li, 2004. Quality Assessment and Validation of the MODIS Global Land Surface Temperature. *International Journal of Remote Sensing*, 25:261-274.
- Wang, X., H. Xie, H. Guan, and X. Zhou, 2007. Different Responses of MODIS-Derived NDVI to Root-Zone Soil Moisture in Arid and Semi-Arid Regions. *Journal of Hydrology*, 340:12-24, doi: 10.1016/j.jhydrol.2007.03.022.
- Wang, X., H. Xie, H. Sharif, and J. Zeitler, 2008. Validating NEXRAD MPE and Stage III Precipitation Products for Uniform Rainfall on the Upper Guadalupe River Basin of the Texas Hill Country. *Journal of Hydrology*, 348(1-2):73-86.
- Weissling, B.P., H. Xie, and K. Murray, 2008. Evaluation of NRCS Curve Number and MODIS Time-Series Proxies for Antecedent Moisture Condition. *Civil Engineering and Environmental Systems*, 26(1):85-101, doi: 10.1080/10286600802005356.
- Xie, H., X. Zhou, E. Vivoni, J. Hendrickx, and E. Small, 2005. GIS Based NEXRAD Precipitation Database: Automated Approaches for Data Processing and Visualization. *Computers and Geosciences*, 31(1):65-76.
- Xie, H., X. Zhou, J.M.H. Hendrickx, E.R. Vivoni, H. Guan, Y.Q. Tian, and E. Small, 2006. Evaluation of NEXRAD Stage III Precipitation Data Over a Semiarid Region. *Journal of the American Water Resources Association*, 42:237-256.
- Young, C.B., A.A. Bradley, W.F. Krajewski, A. Kruger, and M. Morrissey, 2000. Evaluating NEXRAD Multisensor Precipitation Estimates for Operational Hydrologic Forecasting. *Journal of Hydrometeorology*, 1:241-254.
- Zarco-Tejada, P.J., C.A. Rueda, and S. Ustin, 2003. Water Content Estimation in Vegetation With MODIS Reflectance Data and Model Inversion Methods. *Remote Sensing of Environment*, 85:109-124.
- Zhou, X., H. Xie, and J. Hendrickx, 2005. Statistical Evaluation of MODIS Snow Cover Products With Constraints From Streamflow and SNOTEL Measurement. *Remote Sensing of Environment*, 94(2):214-231.